Elastic Hamiltonians for quantum analog applications

Choonlae Cho, Sunkyu Yu,* and Namkyoo Park†
Photonic Systems Laboratory, Department of Electrical and Computer Engineering, Seoul National University, Seoul 08826, Korea

(Received 12 February 2019; revised manuscript received 22 March 2020; accepted 24 March 2020; published 16 April 2020)

Elastic waves are complex mixtures of transverse and longitudinal oscillations even in isotropic and homogeneous media, in contrast to the quantum, electromagnetic, or acoustic waves which could share the same formalism of Hamiltonian and application techniques. Here, we reformulate the elastic wave equation into a set of polarization-dependent decoupled Hamiltonians, to enable the quantum analogous techniques for higher functionalities. As an application example, we adopt the supersymmetric transformation from particle physics and apply it to elastic Hamiltonians, for the demonstration of spatial- and polarization-selective separation of guided elastic waves. Enabling the application of quantum-analogous techniques under the established elastic Hamiltonian formulation, our approach provides a pathway for controlling elastic waves, not limited to the control of an individual guided mode for arbitrary elastic waves, demonstrated here with supersymmetric technique.

DOI: 10.1103/PhysRevB.101.134107

I. INTRODUCTION

The similarity between governing equations in different physical systems has repeatedly provided novel perspectives and applications distinct from traditional viewpoints. For example, the reformulation of classical systems in terms of eigenvalue equations sharing the same mathematical form of the Schrödinger equation, often referred to as the quantum-classical analogy [1,2], enables not only the classical simulation of unstable quantum phenomena [3,4] but also quantized wave dynamics and applications in electromagnetics, acoustics, circuitry, etc. Varieties of quantum phenomena and techniques, for example, have been applied toward electromagnetic systems, by reinterpreting the Helmholtz equation in the notion of the Schrödinger equation and then further including the quantum Hall effect and topological theory [5–8], parity-time symmetry and non-Hermitian degeneracy [9], Anderson localization [10], Bloch oscillations [11,12], and supersymmetry (SUSY) [13–17]. In the classical realization of quantum phenomena, the core philosophy lies in the parallelism between a classical governing equation and the quantum mechanical one, e.g., the mathematical equivalence between classical paraxial wave equations and the Schrödinger equation, as demonstrated in electromagnetic [5–7,9–11,13–17] or acoustic [8,12] platforms with simple polarization components.

In the context of classical wave physics, elastic waves hold a unique position due to their tensorial nature, while covering a wide range of length scales from seismic to ultrasonic and to phononic waves [18–25]. One of the critical peculiarities and associated difficulties of elastic waves is in the coexistence of longitudinal (L) and shear (S, or transverse) polarizations, which is in sharp contrast to electromagnetic and acoustic waves having solely transverse or longitudinal polarizations. This coexistence of elastic polarizations (L and S) could offer a wider pathway for increased information delivery. For example, access to the scattering information of both polarizations along with intricate time-domain signal processing enables the acquisition of more accurate information on structural landscapes. To make use of polarization diversity of elastic waves, polarization control techniques for *plane waves*, such as oblique diffraction [26,27], modes interaction via anisotropic media [28], transmodal coupling [29], shear wave splitting [30], and double zero indices [31], have been demonstrated.

Nevertheless, in terms of sharing analogies and techniques between classical and quantum wave systems, the tensorial complexity of the elastic wave equation has hindered its transformation toward the scalar equations analogous to the Schrödinger equation. While it is known that the classical wave equation can be mapped to the Schrödinger equation form [2], this reformulation especially for spatially *guided* elastic waves with separation of L and S polarizations has not been elaborated before, prohibiting the elastic-regime application of quantum-inspired physics and functionalities.

In this paper, we reformulate elastic wave equations to have the same form of the Schrödinger equation, and develop the concept of polarization-dependent *elastic Hamiltonians*—paving a route toward the application of quantum derived techniques for the elastic wave. As an example, out of vast application scenarios of quantum-analogous techniques to elastic waves, we then apply the SUSY ladder [13,14] to elastic Hamiltonians. The control of an individual guided mode for an arbitrary elastic wave input is archived, with perfect (spatial *and* polarization) modal selectivity, where the spatial-mode annihilation and polarization filtering are independently realized. For the material realization of the SUSY ladder, L- and S-polarization-dependent elastic potentials are

*skyu.photon@gmail.com
†nkpark@snu.ac.kr

constructed using the simplest template of a perforated elastic metamaterial. A scalar elastic Hamiltonian based theoretical design providing perfect agreement with the tensorial full-wave numerical verification, our formalism of quantum-analogous elastic Hamiltonians will provide a pathway for handling elastic waves, enabling a quantum-elastic analogy [32] not limited to extended modal control based on SUSY ladders.

II. RESULTS

A. Quantum analogous elastic Hamiltonians

A small-amplitude elastic wave in an inhomogeneous medium is described by the linearized equation [33]

$$\rho\frac{\partial^2\mathbf{u}}{\partial t^2} = (\lambda + \mu)\nabla(\nabla\cdot\mathbf{u}) + \mu\nabla^2\mathbf{u} + \nabla\lambda\,(\nabla\cdot\mathbf{u}) + \nabla\mu\times(\nabla\times\mathbf{u}) + 2(\nabla\mu\cdot\nabla)\mathbf{u}, \quad (1)$$

where $\mathbf{u}$ is the particle displacement vector, ρ is medium density, and λ and μ are Lamé's first and second parameters, respectively. To develop the elastic Hamiltonian formalism for the elastic wave, by following [1,2], we consider a wave of frequency ω propagating along the z axis, in a medium allowing the one-dimensional material variations of $\rho=\rho(x)$, $\lambda=\lambda(x)$, and $\mu=\mu(x)$. Expanding Helmholtz's theorem to an inhomogeneous elastic medium [34,35], the in-plane elastic wave then is decomposed into the irrotational L-polarization mode $\mathbf{u}_\mathrm{L}=[\mathbf{u}_{\mathrm{L}x}(x)\boldsymbol{x}+\mathbf{u}_{\mathrm{L}z}(x)\mathbf{z}]e^{i(\omega t-kz)}$ with $\nabla\times\mathbf{u}_\mathrm{L}=0$ and the solenoidal S-polarization mode $\mathbf{u}_\mathrm{S}=[\mathbf{u}_{\mathrm{S}x}(x)\boldsymbol{x}+\mathbf{u}_{\mathrm{S}z}(x)\mathbf{z}]e^{i(\omega t-kz)}$ with $\nabla\cdot\mathbf{u}_\mathrm{S}=0$. Each polarization mode then satisfies

$$-\rho\omega^2\mathbf{u}_\mathrm{L} = (\lambda+\mu)\nabla(\nabla\cdot\mathbf{u}_\mathrm{L}) + \mu\nabla^2\mathbf{u}_\mathrm{L} + \frac{d\lambda}{dx}(\nabla\cdot\mathbf{u}_\mathrm{L})\boldsymbol{x} + 2\frac{d\mu}{dx}(\mathbf{x}\cdot\nabla)\mathbf{u}_\mathrm{L}, \quad (2)$$

$$-\rho\omega^2\mathbf{u}_\mathrm{S} = \mu\nabla^2\mathbf{u}_\mathrm{S} + \frac{d\mu}{dx}\boldsymbol{x}\times(\nabla\times\mathbf{u}_\mathrm{S}) + 2\frac{d\mu}{dx}(\boldsymbol{x}\cdot\nabla)\mathbf{u}_\mathrm{S}, \quad (3)$$

where vectorial Eqs. (2) and (3) provide the self-contained, decoupled scalar equations for $\mathbf{u}_{\mathrm{L}z}(x)$ and $\mathbf{u}_{\mathrm{S}x}(x)$:

$$-\rho\omega^2 u_{\mathrm{L}z} = (\lambda+2\mu)\left[\frac{d^2u_{\mathrm{L}z}}{dx^2} - k^2u_{\mathrm{L}z}\right] + 2\frac{d\mu}{dx}\frac{du_{\mathrm{L}z}}{dx}, \quad (4)$$

$$-\rho\omega^2 u_{\mathrm{S}x} = \mu\left[\frac{d^2u_{\mathrm{S}x}}{dx^2} - k^2u_{\mathrm{S}x}\right] + 2\frac{d\mu}{dx}\frac{du_{\mathrm{S}x}}{dx}. \quad (5)$$

From Eqs. (4) and (5), the transformations of $u_{\mathrm{L}z}(x)=\psi^\mathrm{L}(x)/\exp[\int(d\mu/dx)(\lambda+2\mu)^{-1}dx]$ and $u_{\mathrm{S}x}(x)=\psi^\mathrm{S}(x)/\mu$ for the removal of the first-order derivative terms then lead

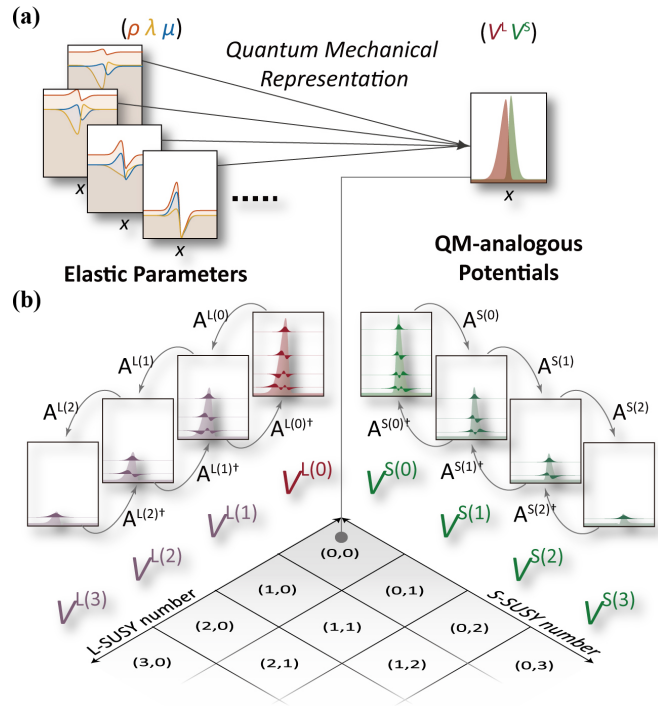

FIG. 1. Quantum-analogous potential description of elastic materials and application of the SUSY transformations. (a) Inhomogeneous elastic media defined by three wave parameters (ρ, λ, and μ) and their elastic potential landscape representation (V^L, V^S) each for L and S polarizations. (b) Illustration of SUSY-transformed elastic potentials and their successive ground-state annihilations for each L- and S-polarization axis. These SUSY transformations on V^L and V^S are independent of each other.

to the polarization-dependent elastic eigenvalue equations $[-d^2/dx^2+V^{\mathrm{L,S}}(x)]\psi^{\mathrm{L,S}}=-k^2\psi^{\mathrm{L,S}}$, each for the L and S waves. Comparing these equations to Schrödinger equations, we now *define* the *elastic Hamiltonian operators* $H^{\mathrm{L,S}}=-d^2/dx^2+V^{\mathrm{L,S}}(x)$ with *elastic potentials* $V^{\mathrm{L,S}}(x)$:

$$V^\mathrm{L}(x) = -\omega^2n_\mathrm{L}^2(x) - \frac{\mu'(\lambda+\mu)'}{(\lambda+2\mu)^2} + \frac{\mu''}{\lambda+2\mu}, \quad (6)$$

$$V^\mathrm{S}(x) = -\omega^2n_\mathrm{S}^2(x) + \frac{\mu''}{\mu}, \quad (7)$$

where $n_\mathrm{L}(x)=[\rho/(\lambda+2\mu)]^{1/2}$ and $n_\mathrm{S}(x)=(\rho/\mu)^{1/2}$ are the refractive indices for L and S modes, respectively, and $f'(x)$ denotes the x derivative of $f(x)$. It is noted that the remaining components of $\mathbf{u}_\mathrm{L}$ and $\mathbf{u}_\mathrm{S}$, i.e., $u_{\mathrm{L}x}(x)$ and $u_{\mathrm{S}z}(x)$, also can be derived from $u_{\mathrm{L}z}(x)$ and $u_{\mathrm{S}x}(x)$ using Eqs. (2) and (3), respectively. See also note S1 in Supplemental Material [36] for the derivation of the elastic potential $V^\mathrm{F}(x)$ for the flexural polarization mode $u_\mathrm{F}=[u_{\mathrm{F}y}(x)\boldsymbol{y}]e^{i(\omega t-kz)}$.

Of practical importance for the above set of polarization-dependent elastic Hamiltonians is in the individual control of L and S waves with the introduction of two *independent* potential landscapes $V^\mathrm{L}(x)$ and $V^\mathrm{S}(x)$, which are mapped from the set of three elastic parameters (ρ, λ, μ) [Fig. 1(a); see note S2 in [36] for details]. With elastic Hamiltonian operators and elastic scalar potentials as defined above, it is

now straightforward to implement quantum-classical analogies, such as parity-time symmetry [9], adiabatic passage [10], Bloch oscillation [11], and Anderson localization [37] toward elastic waves. As an example, here, we focus on the elastic application of SUSY quantum mechanics [38] and SUSY photonics [13–17], for the control of an individual guided mode for an arbitrary elastic wave input, which realizes spatial- and polarization-mode selectivity.

B. SUSY transformation of elastic Hamiltonians

The formalism of the SUSY (or Darboux) transformation [38] is based on the factorization of the Hamiltonian operator, enabling analytic and deterministic construction of wave potentials with quasi-isospectral spectra. For the *original* Hamiltonian $H^{(0)} = -d^2/dx^2 + V^{(0)}(x)$ satisfying $H^{(0)}\psi_i{}^{(0)} = -{k_i}^2\psi_i{}^{(0)}$, in which subscript i denotes mode number, the Hermitian adjoint pair $A^{(0)} = -d/dx + W^{(0)}(x)$ and $A^{(0)\dagger} = d/dx + W^{(0)}(x)$ leads to the relation of $H^{(0)} = A^{(0)\dagger}A^{(0)} + E^{(0)}$, where $W^{(0)}$ is the solution of the Riccati equation $dW^{(0)}/dx = -W^{(0)2} + V^{(0)}(x) + E^{(0)}$ for an arbitrary selection of $E^{(0)}$. This allows the introduction of superpartner Hamiltonian $H^{(1)} = -d^2/dx^2 + V^{(1)}(x) = A^{(0)}A^{(0)\dagger} + E^{(0)}$, and corresponding superpartner potential $V^{(1)} = V^{(0)} - 2dW^{(0)}/dx$. For the selection of $E^{(0)} = -{k_0}^2$ [with the Ricatti solution $W^{(0)} = d(\log\psi_0{}^{(0)})/dx$ where $\psi_0{}^{(0)}$ and $-{k_0}^2$ are the ground-state eigenfunction and eigenvalue of $H^{(0)}$], a spectrum of superpartner potential $H^{(1)}$ is identical to that of $H^{(0)}$, except for the ground state (thus quasi-isospectral; see note S3 in [36]). The sequential application of the quasi-isospectral SUSY factorization, such as $H^{(1)} = A^{(1)\dagger}A^{(1)} + E^{(1)}$ which leads to $H^{(2)} = A^{(1)}A^{(1)\dagger} + E^{(1)}$, then accomplishes the sequential annihilation of the lowest eigenmode, which has been applied to selective modal filtering [13,14], real spectra in complex potentials [15], random-wave switching [16], and band-gap material design [17] in photonics (see [36] for the details of the SUSY transformation). We also note that the SUSY transformation provides an exact *analytic* and *deterministic* solution, involving only differentiation and log operation to the original potential [36]. SUSY transformations are also applicable to any finite potential landscapes: some shape invariant potentials such as harmonic, Rosen-Morse, Pöschl-Teller, and Scarf potentials [38] and any arbitrary potential shape even with complex-valued materials [15].

For our case of elastic Hamiltonians $H^{\mathrm{L,S}} = -d^2/dx^2 + V^{\mathrm{L,S}}$, each governing the L and S modes [Fig. 1(a)], the families of the potentials $\{V^{\mathrm{L}(p)}\}$ and $\{V^{\mathrm{S}(q)}\}$ each constitute the SUSY potential landscapes with the annihilation of p lower "longitudinal" spatial modes and q lower "shear" spatial modes [Fig. 1(b)]. One of the prominent applications utilizing the quasi-isospectrality of SUSY transformation is a SUSY *ladder* [13,14]. In Fig. 2, we show an example of a three-level elastic SUSY *ladder*, i.e., *elastic SUSY potential wells evanescent-coupled in series*, which provides ground-state filtering at each coupling stage, from the quasi-isospectral ground-state annihilation. First, for an arbitrary input waveguide having $V^{\mathrm{L}(0)}(x)$ and $V^{\mathrm{S}(0)}(x)$, the superpartner families of elastic SUSY potentials for each polarization $\{V^{\mathrm{L}(p)}\}$ and $\{V^{\mathrm{S}(q)}\}$ [regions in color in Figs. 2(a) and 2(b)] are

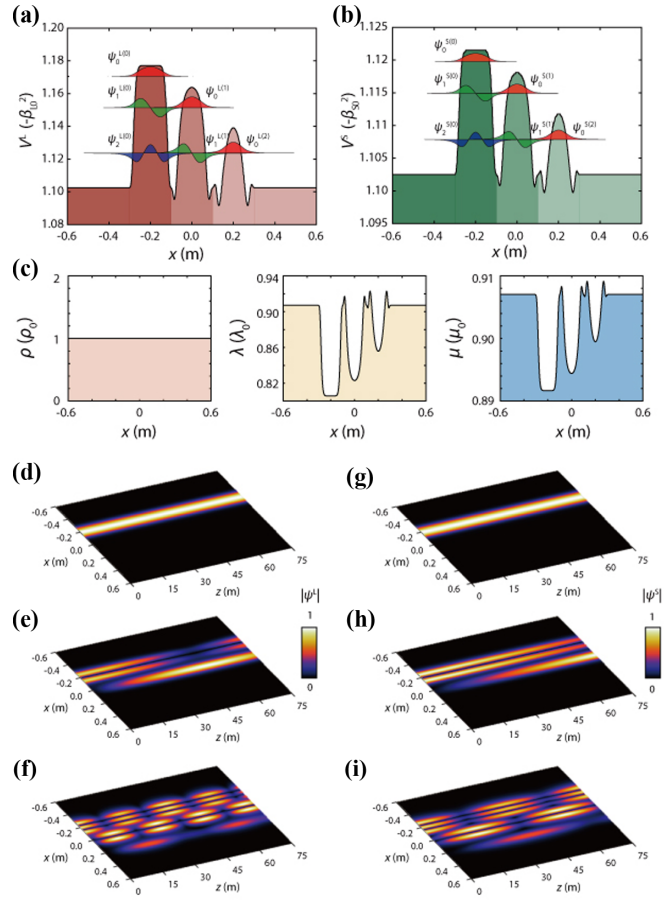

FIG. 2. Polarization-selective SUSY ladders for elastic waves. (a) Longitudinal- and (b) shear-potential landscapes. (a, b) Black lines for SUSY ladder potentials $V^{\mathrm{L}(\Sigma)}$ and $V^{\mathrm{S}(\Sigma)}$. Regions in color are individual SUSY partner potentials $V^{\mathrm{L}(p)}$ and $V^{\mathrm{S}(q)}$ composing SUSY ladders. Here, potentials are normalized to the negative square of propagation constants of a plane wave. Eigenstates of each $V^{\mathrm{L}(p)}$ and $V^{\mathrm{S}(q)}$ are overlaid for lowest, first higher, and second higher modes, in red, green, and blue colors, respectively. (c) Spatial profiles of elastic wave parameters (ρ, λ, and μ) *calculated from* elastic SUSY ladder potentials $V^{\mathrm{L,S}(\Sigma)}$ designed in (a) and (b). To reduce the design freedom, $\rho(x)$ was set to a constant ρ_0. (d–i) Wave propagations through elastic SUSY ladders for the input of different eigenmodes $\psi_i{}^{\mathrm{L,S}(0)}$ to the input waveguide of $V^{\mathrm{L,S}(0)}$ (position centered at $x = -0.2$). Full coupling is achieved between phase-matched eigenstates: (d, g) the ground state $\psi_0{}^{\mathrm{L,S}(0)}$ trapped in the input waveguide of $V^{\mathrm{L,S}(0)}$, (e, h) the first excited state $\psi_1{}^{\mathrm{L,S}(0)}$ of $V^{\mathrm{L,S}(0)}$ penetrating into the adjacent waveguide of first SUSY-partner potential $V^{\mathrm{L,S}(1)}$ of $\psi_0{}^{\mathrm{L,S}(1)}$, and (f, i) the second excited state $\psi_2{}^{\mathrm{L,S}(0)}$ penetrating into waveguides of first and second SUSY-partner potentials $V^{\mathrm{L,S}(1)}$ and $V^{\mathrm{L,S}(2)}$. It is noted that SUSY potentials and eigenmodes here are obtained by using finite difference method with MATLAB, and (ρ, λ, and μ) values in (c) have been normalized to that of aluminum with a plane strain approximation [35] at the target frequency of 200 kHz.

calculated by $V^{(i+1)} = V^{(i)} - 2d^2(\log\psi_0{}^{(i)})/dx^2$. The L- and S-polarization SUSY ladder potentials $V^{\mathrm{L,S}(\Sigma)}(x)$ [black lines in Figs. 2(a) and 2(b)] are then constructed by sequentially placing the obtained SUSY partner potentials in adjacent positions, e.g., $V^{\mathrm{L,S}(i+1)}$ to the right side of $V^{\mathrm{L,S}(i)}$, to

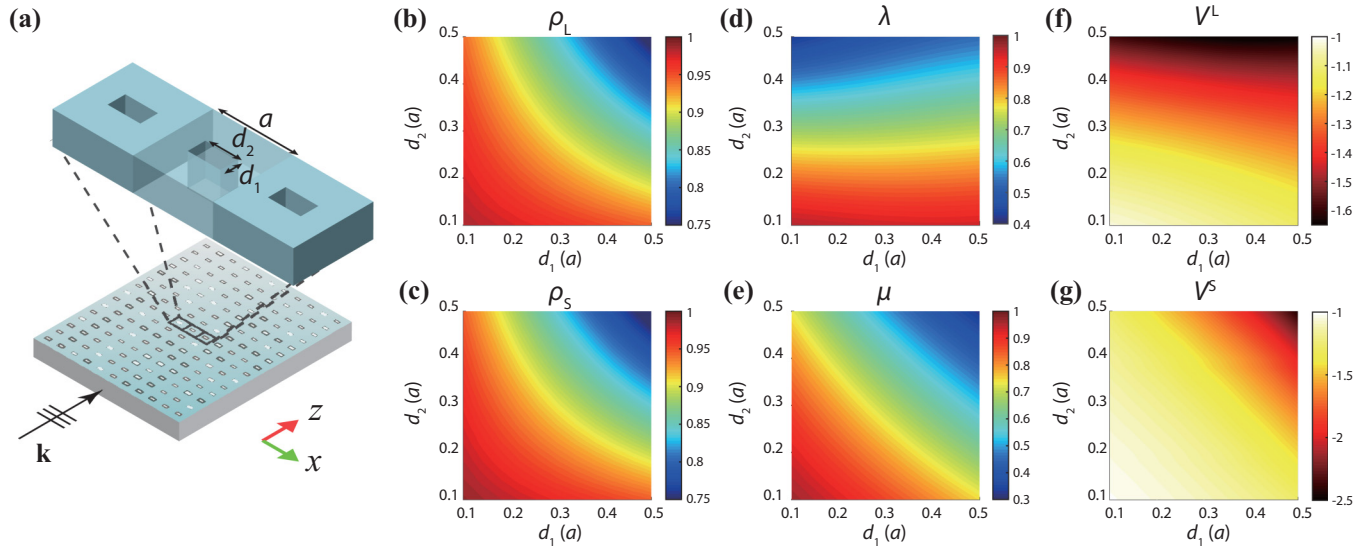

FIG. 3. Elastic metamaterial template for elastic potentials. (a) An illustration of the employed elastic metamaterial, consisting of a square lattice unit cell with a rectangular hole. The lattice constant $a = 1$ mm satisfies the subwavelength conditions of $\sim\Lambda_L/30$ and $\sim\Lambda_S/15$, where Λ_L and Λ_S denote the wavelength of the L and S polarization, respectively, in the Al plate at a 200-kHz frequency. (b–e) FEM (COMSOL) obtained elastic parameters ρ_L, ρ_S, λ, and μ for different hole widths d_1 and d_2. (f, g) Elastic potentials V^L and V^S corresponding to ρ_L, ρ_S, λ, and μ in (b)–(e).

derive evanescent couplings between [14]. The elastic material parameters $\{\rho(x), \lambda(x), \mu(x)\}$ [Fig. 2(c)] as a counterpart of the L- and S-polarization SUSY ladder elastic potentials $V^{L,S(\Sigma)}(x)$ can then be readily derived using analytic Eqs. (S3) and (S4) in [36].

The operation of the SUSY ladder, which is designed from input waveguide potentials $V^{L,S(0)}(x)$ and implemented in terms of elastic parameter $\{\rho(x), \lambda(x), \mu(x)\}$, has been verified using finite element method (FEM) simulation and the COMSOL Multiphysics solid mechanics module. Analogous to the photonic SUSY ladder [14], the successful operation of the elastic SUSY ladder, i.e., demultiplexing of guided elastic modes, is realized for *each* polarization mode [Figs. 2(d)–2(f) for L modes and Figs. 2(g)–2(i) for S modes].

C. Elastic metamaterials and directional SUSY ladders for perfect modal selectivity

For the physical implementation of the elastic SUSY ladder, we use the template of metamaterials. The subwavelength arrangement of metamaterials enables the effective parameter reproduction of continuous and inhomogeneous elastic potential profiles $V^L(x)$ and $V^S(x)$. As the simplest template supporting two different indices for L and S modes, we employ a two-dimensional square aluminum lattice [in Fig. 3(a)] having an anisotropically perforated rectangular hole at the center. Figures 3(b)–3(e) and Figs. 3(f) and 3(g) show the obtained elastic wave parameters (ρ_L, ρ_S, λ, μ) and associated elastic potentials (V^L, V^S), respectively, for different sets of (d_1, d_2). As is clear from the effective medium theory [39], the longitudinal potential V^L is mainly controlled by the transverse hole width d_2, while V^S is dependent on both d_1 and d_2: The mass density ρ depends on the filling ratio, the longitudinal stiffness $C_{11} = \lambda + 2\mu$ mainly depends on the transversal width of the rectangular hole d_2, and the shear stiffness $C_{66} = \mu$ symmetrically depends on d_1 and d_2 (see note S3 in [36] for the retrieval of effective parameters [40,41] and the relations between the L- and S-stiffness and Lamé parameters in anisotropic structures).

Now, with the elastic metamaterial template, the realization of continuous SUSY potentials becomes possible for the implementation of an elastic mode splitter having perfect (spatial and polarization) selectivity. Figure 4(a) shows $V^{L(\Sigma)}(x)$ and $V^{S(\Sigma)}(x)$ *analytically* designed for the polarization-diversified SUSY ladder composed of seven waveguides. For the metamaterial realization of $V^{L(\Sigma)}(x)$ and $V^{S(\Sigma)}(x)$, these analytically designed, continuous potentials are discretized with a 1-mm grid ($\sim\Lambda_L/30 = \Lambda_S/15$), providing well-defined eigenmodes in perfect match with those of analytical results. Figures 4(b) and 4(c) illustrate the corresponding structural parameters (d_1, d_2) and a snapshot of metamaterial structures in the vicinity of each waveguide center.

It is emphasized that, in the design of this *polarization-diversified* SUSY ladder, we assign different directions of spatial demultiplexing for each polarization, i.e., L polarization $V^{L(p+1)}$ positioned to the *left* side of $V^{L(p)}$, and S polarization $V^{S(q+1)}$ positioned to the *right* side of $V^{S(q)}$. For an input of randomly mixed spatial and polarization modes, the polarization-diversified SUSY ladder then separates the L and S polarizations for each assigned direction ($-x$ direction for the L mode and $+x$ direction for the S mode), and sequentially filters each spatial mode upon propagation. Upon propagation, the spatial demultiplexing is achieved by mode-dependent beating, which is determined by coupling coefficients between nearby SUSY potentials. Figure 4(d) shows the temporal evolution of successful demultiplexing for an input wave, obtained from the FEM simulation for the polarization-diversified SUSY ladder employing anisotropically perforated aluminum metamaterial. An excellent agreement has been observed with Fig. 4(e), the finite difference method solution

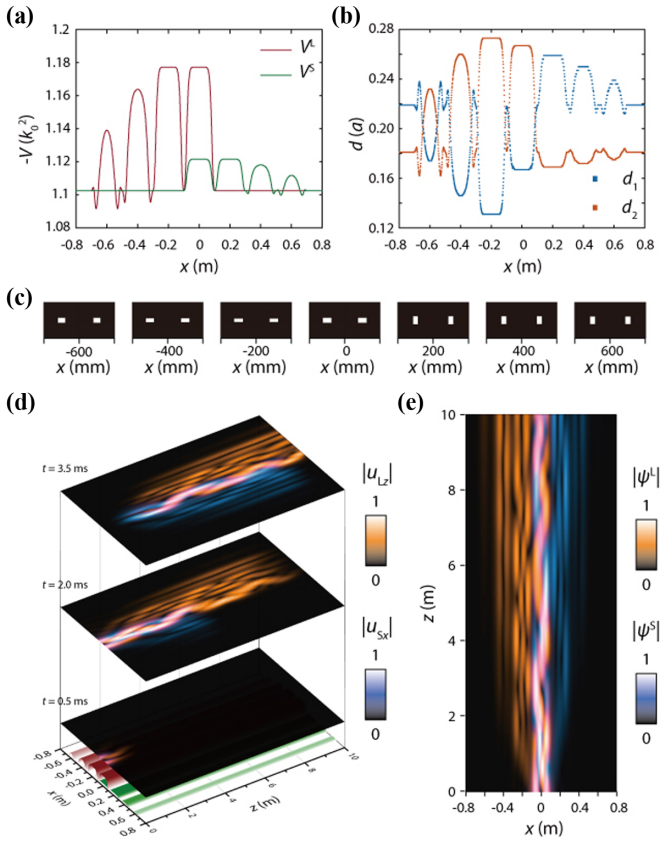

FIG. 4. Design and operation of the polarization-diversified SUSY ladder. (a) The landscapes of elastic potentials for the polarization-diversified SUSY ladders. (b) The structural parameters of elastic metamaterials corresponding to the potentials in (a). (c) Metamaterial structures in the vicinity of each waveguide center. (d) Snapshots of mode splitting for a randomly mixed input of spatial and polarization modes at $t = 0.5$, 2.0, and 3.5 ms. The input of randomly mixed spatial and polarization modes are fed into the input waveguide around $x = 0$, at $t = 0$ ms. For the time domain simulation, the eigenmode expansion method has been used based on FEM (COMSOL Multiphysics) solid mechanics simulation results. (e) The steady-state finite difference method (MATLAB) solution obtained from the analytical scalar elastic Hamiltonians, using the potentials shown in (a).

obtained from the scalar elastic Hamiltonians [Eqs. (4) and (5)] and elastic potentials defined by Eqs. (6) and (7).

It is noted that previous elastic wave control techniques [26–31] have been limited in the polarization manipulation of *plane* waves only. In contrast, we emphasize that our application of the SUSY ladder allows perfect selectivity for an arbitrary (linear combination of both "polarization" and "spatial" multimode) elastic wave input, which has been an impossibility, notably without any penalties in conversion efficiency [14] due to the global phase-matching condition inherited from SUSY [13].

III. CONCLUSION

In summary, by transforming the elastic wave equation into polarization-decoupled scalar elastic Hamiltonians, a direct path for the application of quantum mechanical techniques toward elastic waves is achieved. As a practically important application example, we proposed an elastic SUSY ladder providing perfect modal selectivity, including both "spatial" and "polarization" mode controllability for an arbitrary elastic wave input. The realization of the SUSY ladder with an anisotropically perforated aluminum metamaterial platform proves excellent agreements between theoretical prediction and full-numerical verification. By providing a systematic route to the scalar-equation-based handling of elastic waves, our approach paves the way to direct applications of other diverse quantum-elastic analogies, including parity-time symmetry for elastic modal singularities, Anderson localization for elastic energy focusing, Dirac points for elastic waves, and Zak phases for elastic polarization, not limited to the SUSY transformation demonstrated here for the extended modal capacity.

ACKNOWLEDGMENTS

We acknowledge financial support from the National Research Foundation of Korea through the Global Frontier Program (Grant No. 2014M3A6B3063708). S.Y. was supported by the Basic Science Research Program (Grant No. 2016R1A6A3A04009723).

[1] D. Dragoman and M. Dragoman, *Quantum-Classical Analogies* (Springer, New York, 2013).
[2] P. Sheng, *Introduction to Wave Scattering, Localization and Mesoscopic Phenomena* (Springer, New York, 2006).
[3] X. Zhang, Phys. Rev. Lett. **100**, 113903 (2008).
[4] K. Shandarova, C. E. Rüter, D. Kip, K. G. Makris, D. N. Christodoulides, O. Peleg, and M. Segev, Phys. Rev. Lett. **102**, 123905 (2009).
[5] S. Raghu and F. D. M. Haldane, Phys. Rev. A **78**, 033834 (2008).
[6] A. Kavokin, G. Malpuech, and M. Glazov, Phys. Rev. Lett. **95**, 136601 (2005).
[7] L. Lu, J. D. Joannopoulos, and M. Soljačić, Nat. Photonics **8**, 821 (2014).
[8] C. He, X. Ni, H. Ge, X.-C. Sun, Y.-B. Chen, M.-H. Lu, X.-P. Liu, and Y.-F. Chen, Nat. Phys. **12**, 1124 (2016).
[9] C. E. Rüter, K. G. Makris, R. El-Ganainy, D. N. Christodoulides, M. Segev, and D. Kip, Nat. Phys. **6**, 192 (2010).
[10] T. Schwartz, G. Bartal, S. Fishman, and M. Segev, Nature (London) **446**, 52 (2007).
[11] M. Ben Dahan, E. Peik, J. Reichel, Y. Castin, and C. Salomon, Phys. Rev. Lett. **76**, 4508 (1996).
[12] H. Sanchis-Alepuz, Y. A. Kosevich, and J. Sánchez-Dehesa, Phys. Rev. Lett. **98**, 134301 (2007).
[13] M.-A. Miri, M. Heinrich, R. El-Ganainy, and D. N. Christodoulides, Phys. Rev. Lett. **110**, 233902 (2013).

[14] M. Heinrich, M.-A. Miri, S. Stützer, R. El-Ganainy, S. Nolte, A. Szameit, and D. N. Christodoulides, Nat. Commun. **5**, 3698 (2014).
[15] M.-A. Miri, M. Heinrich, and D. N. Christodoulides, Phys. Rev. A **87**, 043819 (2013).
[16] S. Yu, X. Piao, and N. Park, Phys. Rev. Appl. **8**, 054010 (2017).
[17] S. Yu, X. Piao, J. Hong, and N. Park, Nat. Commun. **6**, 8269 (2015).
[18] M. Maldovan, Nat. Mater. **14**, 667 (2015).
[19] J.-K. Yu, S. Mitrovic, D. Tham, J. Varghese, and J. R. Heath, Nat. Nanotechnol. **5**, 718 (2010).
[20] M. Eichenfield, J. Chan, R. M. Camacho, K. J. Vahala, and O. Painter, Nature (London) **462**, 78 (2009).
[21] D. Mirlin, in *Modern Problems in Condensed Matter Sciences* (Elsevier, Amsterdam, 1982), p. 3.
[22] M. Maldovan, Nature (London) **503**, 209 (2013).
[23] M. J. Lowe, D. N. Alleyne, and P. Cawley, Ultrasonics **36**, 147 (1998).
[24] R. Muthupillai, D. Lomas, P. Rossman, J. F. Greenleaf, A. Manduca, and R. Ehman, Science **269**, 1854 (1995).
[25] J. Virieux and S. Operto, Geophysics **74**, WCC1 (2009).
[26] J. L. Rose, *Ultrasonic Guided Waves in Solid Media* (Cambridge University, Cambridge, England, 2014).
[27] Y. Cho, IEEE Trans. Ultrason. Ferroelectr. Freq. Control **47**, 591 (2000).
[28] A. H. Nayfeh, *Wave Propagation in Layered Anisotropic Media with Applications to Composites* (Elsevier, Amsterdam, 1995).
[29] J. M. Kweun, H. J. Lee, J. H. Oh, H. M. Seung, and Y. Y. Kim, Phys. Rev. Lett. **118**, 205901 (2017).
[30] Z. Chang, H.-Y. Guo, B. Li, and X.-Q. Feng, Appl. Phys. Lett. **106**, 161903 (2015).
[31] F. Liu and Z. Liu, Phys. Rev. Lett. **115**, 175502 (2015).
[32] D. N. Christodoulides, F. Lederer, and Y. Silberberg, Nature (London) **424**, 817 (2003).
[33] F. C. Karal, Jr. and J. B. Keller, J. Acous. Soc. Am. **31**, 694 (1959).
[34] K. Aki and P. G. Richards, *Quantitative Seismology*, 2nd ed. (University Science Books, Sausalito, 2002).
[35] K. F. Graff, *Wave Motion in Elastic Solids* (Courier, New York, 2012).
[36] See Supplemental Material at http://link.aps.org/supplemental/10.1103/PhysRevB.101.134107 for the derivation of the elastic potentials for the flexural polarization mode, details of the SUSY transformation, and Lamé parameters in anisotropic structures.
[37] J. Billy, V. Josse, Z. Zuo, A. Bernard, B. Hambrecht, P. Lugan, D. Clément, L. Sanchez-Palencia, P. Bouyer, and A. Aspect, Nature (London) **453**, 891 (2008).
[38] F. Cooper, A. Khare, and U. Sukhatme, Phys. Rep. **251**, 267 (1995).
[39] Y. Wu, Y. Lai, and Z.-Q. Zhang, Phys. Rev. B **76**, 205313 (2007).
[40] H. J. Lee, H. S. Lee, P. S. Ma, and Y. Y. Kim, J. Appl. Phys. **120**, 104902 (2016).
[41] Y. Lai, Y. Wu, P. Sheng, and Z.-Q. Zhang, Nat. Mater. **10**, 620 (2011).